# $H_2S$ removal and microbial community composition in an anoxic biotrickling filter under autotrophic and mixotrophic conditions

Ramita Khanongnuch[a*], Francesco Di Capua[c], Aino-Maija Lakaniemi[a], Eldon R. Rene[b], Piet N. L. Lens[a, b]

[a]Laboratory of Chemistry and Bioengineering, Tampere University of Technology, P.O. Box 541, 33101 Tampere, Finland

[b]UNESCO-IHE Institute for Water Education, P.O. Box 3015, 2601 DA Delft, The Netherlands

[c]Department of Civil, Architectural and Environmental Engineering, University of Naples Federico II, 80125 Naples, Italy

[*]Corresponding author:

Ramita Khanongnuch

Laboratory of Chemistry and Bioengineering, Tampere University of Technology, P. O. Box 541, 33101 Tampere, Finland

E-mail: ramita.khanongnuch@tut.fi

Tel: +358 442415042

**Abstract**

Removal of $H_2S$ from gas streams using $NO_3^-$-containing synthetic wastewater was investigated in an anoxic biotrickling filter (BTF) at feed N/S ratios of 1.2-1.7 mol $mol^{-1}$ with an initial nominal empty bed residence time of 3.5 min and a hydraulic retention time of 115 min. During 108 days of operation under autotrophic conditions, the BTF showed a maximum elimination capacity (EC) of 19.2 g S $m^{-3}$ $h^{-1}$ and $H_2S$ removal efficiency (RE) above 99%. Excess biofilm growth reduced the HRT from 115 to 19 min and decreased the desulfurization efficiency of the BTF. When the BTF was operated under mixotrophic conditions by adding organic carbon (10.2 g acetate $m^{-3}$ $h^{-1}$) to the synthetic wastewater, the $H_2S$ EC decreased from 16.4 to 13.1 g S $m^{-3}$ $h^{-1}$, while the $NO_3^-$ EC increased from 9.9 to 11.1 g $NO_3^-$-N $m^{-3}$ $h^{-1}$, respectively. *Thiobacillus* sp. (98-100% similarity) was the only sulfur-oxidizing nitrate-reducing bacterium detected in the BTF biofilm, while the increased abundance of heterotrophic denitrifiers, i.e. *Brevundimonas* sp. and *Rhodocyclales*, increased the consumed N/S ratio during BTF operation. Residence time distribution tests showed that biomass accumulation during BTF operation reduced gas and liquid retention times by 17.1% and 83.5%, respectively.

**Keywords:** $H_2S$ removal; autotrophic denitrification; nitrate-containing wastewater; substrate competition; PCR-DGGE

## 1. Introduction

Hydrogen sulfide ($H_2S$) is generated by many industrial activities, livestock operations and anaerobic digestion of wastes [1,2]. It is harmful to human health at 100 $ppm_v$ [3] and causes corrosion to equipment, e.g. pipelines, cogeneration engines and biogas distribution units [4]. Particularly, $H_2S$ needs to be removed from biogas to obtain a high quality, safe and convenient energy source from the anaerobic digestion of organic waste. The $H_2S$ concentrations must be less than 1000 $ppm_v$ for direct combustion of biogas, whereas for the application as a fuel in internal combustion engines or compressed natural gas production (CNG), the $H_2S$ concentration must be less than 100 $ppm_v$ and 16 $ppm_v$, respectively [5].

The use of anoxic biotrickling filters (BTF) for $H_2S$ removal has received widespread industrial attention in the last few decades [4,6] as more environmentally friendly and cost-effective technologies than the conventional physico-chemical methods such as chemical precipitation and scrubbing [7,8]. Anoxic $H_2S$ oxidation via autotrophic denitrification proceeds according to Eq. (1) and (2) by sulfur-oxidizing nitrate-reducing (SO-NR) bacteria [9]:

$$HS^- + 1.23\ NO_3^- + 0.093\ NH_4^+ + 0.438\ HCO_3^- + 0.573\ H^+ + 0.027\ CO_2 \rightarrow 0.093\ C_5H_7O_2N + 0.614\ N_2 + SO_4^{2-} + 0.866\ H_2O \quad (1)$$

$$HS^- + 0.350\ NO_3^- + 0.013\ NH_4^+ + 0.059\ HCO_3^- + 1.4\ H^+ + 0.004\ CO_2 \rightarrow 0.013\ C_5H_7O_2N + 0.175\ N_2 + S^0 + 1.21\ H_2O \quad (2)$$

In recent years, $H_2S$ removal in anoxic BTFs with recycling of the liquid medium has been studied at the laboratory-scale. In these studies, the authors have tested the performance of the BTF under the influence of different parameters and operational strategies such as the use of different packing materials, gas-liquid flow patterns, mode of reactor start-up and the effect of inlet $H_2S$ concentrations (Table 1). When $NO_3^-$ is supplied in batch feeding mode, the $H_2S$ RE decreases once $NO_3^-$ is completely consumed [4,7]. This leads to $H_2S$ fluctuations

during BTF operation which affects the stability of the BTF performance during long-term operation. Continuous $NO_3^-$ supply can be applied to overcome the fluctuations typically observed in $H_2S$ removal during BTF operation and reduce stress on microbial population due to $NO_3^-$ starvation during discontinuous dosing [10]. López et al. [11] showed that a feedforward control of $NO_3^-$ dosing significantly reduces the impact of $H_2S$ load fluctuation to the anoxic BTF performance, resulting in stable $H_2S$ removal. In contrast, Li et al. [12] observed no significant effects of the $NO_3^-$ supplying strategy on $H_2S$ removal at N/S ratios ranging from 0.25 to 1.0 and a constant $H_2S$ concentration of ~1600 $ppm_v$. Additional research on the effects of $H_2S$ concentration, N/S ratio and microbial community composition on anoxic desulfurization in BTF are still required.

**Table 1.**

Using chemical nitrate sources (e.g. $NaNO_3$ and $KNO_3$) increases the operating costs [13]. Hence, a continuous system for $H_2S$ removal from gas stream (e.g. biogas) using nitrified/$NO_3^-$-containing wastewater would be a sustainable option, particularly if the $H_2S$ treatment plant is located nearby a nitrification bioreactor [13]. Since, some nitrified/$NO_3^-$ contaminated wastewaters such as swine wastewaters, and effluents from nitrification units or fecal sludge treatment [14–17] can also contain residual organics, the effect of organic compound on the performance of a BTF relying on the activity of autotrophic microorganisms needs to be investigated. The main objective of this study was to evaluate the capability of an anoxic BTF for $H_2S$ removal with continuous $NO_3^-$ feeding under autotrophic and mixotrophic conditions at (i) different $H_2S$ concentrations (from 100 to 500 $ppm_v$), (ii) different N/S ratios (1.2 and 1.7 mol $mol^{-1}$), and (iii) a feed acetate ($CH_3COO^-$) concentration of (51.4 ± 2.8 mg $L^{-1}$).

## 2. Materials and methods

### *2.1. Synthetic nitrified wastewater*

The synthetic nitrified wastewater used as the BTF medium had the following chemical composition (per liter): 0.07-0.46 g $KNO_3$, 1 g $NaHCO_3$, 0.2 g $KH_2PO_4$, 0.1 g $NH_4Cl$, 0.08 g $MgSO_4 \cdot 7H_2O$, 1 mL $FeSO_4 \cdot 7H_2O$ solution and 0.2 mL of trace element solution as described by Zou et al. [18]. Sodium acetate (230 g $CH_3COONa \cdot 3H_2O$ $L^{-1}$) was added as a model organic compound during the mixotrophic operation due to its ease of use and measurement. The pH of the synthetic wastewater was adjusted to ~7.0 with 37% HCl.

### *2.2. Source of inoculum and immobilization of biomass in the BTF*

The inoculum was biofilm-attached K1 carriers (2.17 ± 0.15 VSS $carrier^{-1}$ and VSS/TSS ratio of 0.76) collected from a *Thiobacillus*-dominated lab-scale moving bed biofilm reactor (MBBR) previously operated for anoxic thiosulfate ($S_2O_3^{2-}$) oxidation [19]. The inoculation was performed in a 5-L Schott-Duran bottle filled with 1.5 L of the polyurethane foam (PUF) cubes and 80 pieces of biofilm-attached K1 carriers. The bottle was filled with 3 L medium with 650 mg $S_2O_3^{2-}$-S $L^{-1}$ and 140 mg $NO_3^-$-N $L^{-1}$, respectively, and purged with $N_2$ gas for 10 min. After 14-d incubation at room temperature (22 ± 2 °C), the incubated PUF cubes were mixed with new PUF cubes and added to the BTF to obtain a bed height of 30 cm.

### *2.3. Bioreactor set-up and operation*

The laboratory-scale BTF used in this study (Fig. 1) was made of glass (Glass discovery, The Netherlands) and had an inner diameter and a bed height of 12 and 30 cm, respectively. The BTF packed-bed comprised of 264 pieces of PUF cubes (BVB Substrate, The Netherlands) with a cube size of 8 $cm^3$, a void ratio of 0.98 and a density of 28 kg $m^{-3}$, corresponding to total bed volume of 2.11 L occupied by PUF.

**Fig. 1.**

The gas stream fed to the BTF consisted of a mixture of $N_2$ gas and $H_2S$ generated using solutions of $Na_2S$ (0.1-0.3 N) and $H_2SO_4$ (1 N). The desired $H_2S$ concentrations were obtained by controlling $Na_2S$ concentrations and dripping rates using a peristaltic pump (Cole-Parmer, USA). The gas stream was fed to the BTF in counter-current mode, controlled by a Delta Smart II Mass Flow controller (Brooks instrument, USA) connected to a flow meter. The gas flow rate was maintained at 60 L $h^{-1}$, corresponding to a theoretical empty bed residence time (EBRT) of 3 min. The synthetic wastewater and recirculated effluent were fed to the BTF from the top at a flow rate of 10 L $d^{-1}$ and 50 L $d^{-1}$ (Masterflex, Cole-Parmer, USA), respectively, to obtain a total trickling liquid flow rate of 60 L $d^{-1}$. The residence time distribution (RTD) test was performed to estimate the nominal residence times of the gas-phase $H_2S$ (EBRT) and liquid medium (hydraulic retention time, HRT) of the BTF before and after the experiments (days -16 and 139, respectively). The RTD test and data analysis were performed according to the procedure described by Fogler [20]. The Bodenstein number (*Bo*) to characterize the axial dispersion in the BTF was determined based on the RTD test data (see the Supplementary material).

The BTF was operated for 154 d in five different experimental phases (P1, P2, P3, P4 and P5) at a temperature of 24 (±1) °C (Table 2). In phase P1, the BTF was filled with 4 L of the synthetic wastewater containing initial concentrations of 67.4 (±8.4) mg $S_2O_3^{2-}$-S $L^{-1}$ and 15.5 (±1.0) mg $NO_3^-$-N $L^{-1}$ and operated in batch mode for 11 d (days -15 to 0) to allow biofilm formation on the PUF cubes. From day 1 onwards (phase P2), the retaining synthetic wastewater was drained out from the BTF. The gas stream containing $H_2S$ and the synthetic wastewater were continuously fed to the BTF. The inlet $H_2S$ concentration in phase P2 was 111 (±15) $ppm_v$ and was increased to 434 (±28) $ppm_v$ from phase P3 onwards. $NO_3^-$ concentrations were gradually increased from 12.2 (±2.1) mg $NO_3^-$-N $L^{-1}$ in phase P2 to 62.1 (±2.0) mg $NO_3^-$-N $L^{-1}$ in phase P5 (Table 2). In phase P5, acetate was added to the synthetic

wastewater at a concentration of 51.4 (±2.8) mg $L^{-1}$. Sulfur, nitrogen and carbon mass balances (Table S1) were performed based on the experimental data obtained during 3 days of steady-state observed in each experimental phase. Data from both gas and liquid phases were considered for sulfur and carbon mass balances, while nitrogen mass balance was based only on the liquid phase.

**Table 2.**

*2.4. Batch activity tests*

Batch tests were performed at the end of each experimental phase to determine the SO-NR activity of the biomass attached on the PUF cubes. Tests I, II and III were conducted under autotrophic conditions with biomass collected during phases P3, P4 and P5 of BTF operation, respectively (Table 3). In addition, biomass collected during phase P5 was also tested with acetate in the medium (test IV). Three pieces of PUF cubes collected from the BTF were immediately cut into small pieces (2×0.67×0.67 $cm^3$) using a sterile surgical blade and divided into two 250-mL batch bottles (working volume of 200 mL), resulting in a total PUF volume of 12.1 (±0.6) $cm^3$ per bottle. $Na_2S·9H_2O$ was added as the sulfide source to the synthetic nitrified wastewater. The bottles were purged with $N_2$ gas to ensure anoxic conditions and incubated at 22 (±2) °C and 65 rpm mixing.

**Table 3.**

*2.5. Microbial community analysis*

Two pieces of PUF cubes were collected from the BTF at the end of each experimental phase (days 9, 25, 72, 112, and 138) for the microbial community analysis using polymerase chain reaction-denaturing gradient gel electrophoresis (PCR-DGGE) as described by Khanongnuch et al. [21]. The procedure of PCR-DGGE including DNA extraction and sequencing are described in the Supplementary material.

*2.6. Analytical methods*

The liquid samples were filtered through 0.45 µm syringe filters (Sigma-Aldrich, USA) prior measurement of $NO_3^-$, $S_2O_3^{2-}$ and $SO_4^{2-}$ concentrations using ion chromatography with a Dionex ICS-1000 (Thermo Fisher, USA) as described by Villa-Gomez et al. [22]. The pH of the solutions was measured using a Präzision-pH-Meter E510pH (Metrohm, Switzerland) equipped with a SenTix 21 pH electrode (WTW, Germany). The concentrations of total sulfide ($S^{2-}$), nitrite ($NO_2^-$) and COD were measured using colorimetric methods [23] with a Lamda 365 UV/VIS spectrophotometer (Perkin-Elmer, USA). Alkalinity was measured by potentiometric titration using a Titrino plus 848 titration meter equipped with a Metrohm 801 Stirrer (Metrohm AG, Switzerland). Acetate concentrations were measured using a Varian 430-GC gas chromatograph (Varian Inc., USA) as described by Eregowda et al. [24]. Gas composition ($CH_4$, $CO_2$ and $N_2$) was measured using a SCION 456-GC gas chromatograph as described in the Supplementary material. $H_2S$ and $O_2$ concentrations in the gas phase were measured using a Dräger X-am® 7000 gas detector (Dräger, Germany).

*2.7. Data analysis*

The statistical differences in the performance parameters during each phase of BTF operation, i.e. EC and RE, were determined using a one-way analysis of variance (ANOVA) in combination with Tukey's multiple comparison test (Minitab Inc., USA). The significant difference was considered at 95% ($P \leq 0.05$).

**3. Results**

*3.1. $H_2S$ and $NO_3^-$ degradation behavior in the anoxic BTF*

At the start of the experiments (day -16), based on the results of the RTD test the mean residence times of gas (EBRT) and liquid (HRT) in the BTF were 3.5 and 115 min, respectively (Fig. S1 and S2). The initial Bodenstein number (*Bo*) in the BTF was 11.4, indicating a near typical plug-flow behavior (*Bo* >10) [25]. However, EBRT and HRT had

decreased to 2.9 and 19 min, respectively, by the end of the experiment (Fig. S1 and S2). As a result, *Bo* decreased to 9.4, which indicates that an axial dispersion of the gas phase, i.e. a nonuniform velocity profile, occurred in the BTF at the end of this study.

During phase P1 (days -15-0), the initial biofilm formation occurred and the obtained $S_2O_3^{2-}$ and $NO_3^-$ RE were 65.2% and 94.2%, respectively (Fig. 2c and e). The effluent pH increased from 7.2 to 7.8 between day -15 and day -13 and thereafter it gradually decreased to 7.0 (Fig. 2a). In phase P2 (days 1-22), the $H_2S$ feed was 111 (±15) $ppm_v$, corresponding to an inlet loading rate (IL) of 3.5-5.6 g S $m^{-3}$ $h^{-1}$ and a N/S ratio of 1.18. The $H_2S$ RE reached 100%, whereas the $NO_3^-$ RE fluctuated between 26 and 82%. $NO_2^-$ concentration, which was 22 mg $NO_2^-$-N $L^{-1}$ on day 0 and the concentration gradually decreased to 2.5 mg $NO_2^-$-N $L^{-1}$ by day 22. In phase P2, approximately 40% of the feed $NO_3^-$ was converted to $N_2$ (Fig. 3b). During phase P2, the effluent pH was 8.5 (±0.3) and the effluent alkalinity concentration decreased from 555 mg $HCO_3^-$ $L^{-1}$ (day 1) to 188 mg $HCO_3^-$ $L^{-1}$ (day 22, Fig. 2b).

**Fig. 2.**

**Fig. 3.**

In phase P3 (days 23-84), the inlet $H_2S$ was increased to 434 (±28) $ppm_v$ (IL of 14.6-19.3 g S $m^{-3}$ $h^{-1}$), while $NO_3^-$ was kept constant (feed N/S ratio of 1.21). The effluent alkalinity was 269 (±37) mg $HCO_3^-$ $L^{-1}$, while pH remained stable at 7.9 (±0.2) from phase P3 onwards (Fig. 2a). During days 25-50, the $H_2S$ RE was 98.2 (±2.6)%, and a maximum elimination capacity (EC) of 19.2 g S $m^{-3}$ $h^{-1}$ was achieved on day 42. The consumed N/S ratio was 1.15 (±0.06) and 11.2% of the fed $H_2S$ was partially oxidized to $S^0$ (Fig. 3). During days 51-66, the BTF was not monitored due to technical problems with the gas detector. Subsequently, the $H_2S$ RE fluctuated in a range of 58-85% and the $H_2S$ EC (12.4 ±1.8 g S $m^{-3}$ $h^{-1}$) was lower than that in phase P2 (Fig. 4a), while the $NO_3^-$ RE was >96% during days 67-83 (Fig. 2c and e). The consumed N/S ratio (1.60 ± 0.23) was higher than the one observed during days 25-

50 (Fig. 3). $NO_2^-$ was not detected in the effluent (<1 mg $NO_2^-$-N $L^{-1}$) from phase P3 onwards (Fig. 2e).

**Fig. 4.**

To recover the $H_2S$ RE that decreased during days 67-83 (phase P3), the influent $NO_3^-$ IL was increased from 9.2 (±0.55) (phase P3) to 12.3 (±0.4) g N $m^{-3}$ $h^{-1}$ in phase P4 (Table 2). As a result, the average $H_2S$ RE increased to 91.9 (±3.7)% (EC of 16.4 ± 2.7 g S $m^{-3}$ $h^{-1}$), while the $NO_3^-$ RE slightly decreased to 82.1 ± 3.7% (days 85-108, Fig. 2d). However, increasing $NO_3^-$ IL increased the EC from 8.6 (±0.6) in phase P3 to 10.0 (±0.7) g N $m^{-3}$ $h^{-1}$ in phase P4. $NO_3^-$ was partially reduced to $NO_2^-$ (Table S1) and the estimated $N_2$ production (75%) was lower compared to phase P3 and P5 (Fig. 3). Compared to the biomass taken from the BTF on day 83 (phase 3), the biomass collected on day 108 resulted in 2.7 and 12.8 times higher $S^{2-}$ and $NO_3^-$ removal rates, respectively (Table 3).

During phase P5, the feed acetate (10.2 g $m^{-3}$ $h^{-1}$) was completely removed from the first day of the addition (Fig. 2f). However, the $H_2S$ RE decreased from 96.0% on day 113 to 67.3% on day 116. The $NO_3^-$ RE and the maximum EC of the BTF in phase P5 were 96.5 (±3.8)% and 11.1 (±3.2) g $NO_3^-$-N $m^{-3}$ $h^{-1}$ (day 134), respectively. The effluent alkalinity increased from 290 (±18) mg $HCO_3^-$ $L^{-1}$ (phase P4) to 366 (±33) mg $HCO_3^-$ $L^{-1}$ (phase P5) and the carbon production rate in the effluent of both gas and liquid phases increased to much higher values than those of the influent (Fig. 3b). In batch tests conducted with biomass collected from phase P5 (day 137), the test without acetate addition (Table 3, test III) showed ~4 times lower specific $NO_3^-$ removal rates compared to the test with acetate addition (Table 3, test IV). Besides, the specific $S^{2-}$ removal rate in the test without acetate (1131 ± 10 g S $m^{-3}_{PUF}$ $h^{-1}$) was slightly higher than the test with acetate (1061 ± 35 g S $m^{-3}_{PUF}$ $h^{-1}$) (Table 3).

*3.2. Microbial community in the BTF*

The microbial community composition demonstrated by a DGGE profile showed an increase of in the number of DGGE bands during the BTF operation (Fig. 5). Bacteria having 98-100% similarity to *Thiobacillus* sp. (bands 1, 9, 10, 12, 13, and 16) were dominant in the DGGE profiles of all experimental phases. The DGGE and sequencing results also indicated that *Stenotrophomonas* sp. (bands 3 and 14) and *Rhodobacter* sp. (bands 4, 15, and 17) were present in the culture during all the experimental phases of the BTF operation (Fig. 5). Conversely, *Chryseobacterium* sp. (band 6) was observed only in the beginning (day 1). From day 84 onwards (the end of phase P3), the new DGGE bands were observed in the DGGE profile, i.e. *Brevundimonas* sp. (band 2), *Rhodocyclales* bacterium (band 11) and *Bacteroidetes* bacterium (bands 7 and 8).

**Fig. 5.**

## 4. Discussion

*4.1. Effect of N/S ratio and organic carbon addition on $H_2S$ removal in the anoxic BTF*

The maximum $H_2S$ EC of 19.2 g S $m^{-3}$ $h^{-1}$ (99% RE) obtained in this study was higher than the EC values reported in anoxic BTFs packed with lava rock (9.1 g S $m^{-3}$ $h^{-1}$) [6] and plastic fibers (11.7 g S $m^{-3}$ $h^{-1}$) [4], which were operated at ILs ranging from 2.0 to 23.5 g S $m^{-3}$ $h^{-1}$. However, the $H_2S$ EC in our study was lower than those observed in anoxic BTFs using open-pore PUF [7,26], pall ring [27] and concrete waste [28] (Table 1) as the packing material. In literature, BTFs in those studies were operated at very high $H_2S$ IL (up to 200 g S $m^{-3}$ $h^{-1}$) and a temperature of 30 °C, which is optimal for the activity of *Thiobacillus* sp. [29]. As the EC trends during stable BTF operation (phase P1, P2 and P3) were very close to the 100% performance line (Fig. 4a), probably higher ECs could still be attained if higher ILs were applied.

The complete $H_2S$ oxidation to $SO_4^{2-}$ in the presence of $NO_3^-$ as the electron acceptor (Eq. 1) results in the production of 1.26 g $SO_4^{2-}$/g $NO_3^-$ (stoichiometric N/S ratio of 1.2 mol $mol^{-1}$), whereas 1.47 g $S^0$/g $NO_3^-$ (stoichiometric N/S ratio of 0.35) is produced during partial $H_2S$ oxidation to elemental sulfur (Eq. 2). In this study, $SO_4^{2-}$ was the main oxidation product during the entire BTF operation and its concentration in the effluent was close to the stoichiometric $SO_4^{2-}$ production (Eq. 1). Jaber et al. [28] studied anoxic biofilters packed with concrete waste at N/S ratios between 0.4 and 1.6 and observed that 55-57% of the inlet $H_2S$ was oxidized to $SO_4^{2-}$ at all tested N/S ratios. Other studies reported that systems operated at N/S ratios > 1.6 mainly produce $SO_4^{2-}$ ($S^0$ production < 15%), while $S^0$ production in the range of 50-70% is typically observed at N/S ratios < 0.7 [7,27,30].

The addition of organic carbon in the form of acetate (phase P5) led to mixotrophic conditions in the BTF which resulted in insufficient $NO_3^-$ availability for $H_2S$ removal by autotrophs. Conversely, acetate addition had a positive effect on $NO_3^-$ removal, as the residual $NO_3^-$ present in phase P4 was almost completely consumed via heterotrophic denitrification during phase P5 (Figs. 2 and 3b). The batch activity tests also showed no substantial difference in the sulfide oxidation activity of the biomass cultivated in the BTF with and without acetate supplementation (Table 3 and Fig. 6). This indicates that SO-NR bacteria were not inhibited by the growth of heterotrophic denitrifiers and were abundantly present in the BTF biofilm during phase P5, as confirmed by the microbial community composition on day 138 (Fig. 5). The consumption of residual $NO_3^-$ at the beginning of phase P5 occurred simultaneously with a decrease in $H_2S$ RE (day 116), indicating the fact that a shortage of $NO_3^-$ decreased the desulfurization efficiency under mixotrophic conditions. Besides acting as an electron donor for denitrification, acetate addition also increases the alkalinity of the reactor (1.60 g $HCO_3^-$/g $NO_3^-$) according to the following equation [31]:

$NO_3^- + 0.63CH_3COO^- + 0.37CO_2 \rightarrow 0.5N_2 + 0.13H_2O + 1.63HCO_3^-$ (3)

During phase P5, heterotrophic denitrification using acetate produced a large amount of alkalinity and $CO_2$ (Table 2), which act as a buffer and inorganic carbon source for the autotrophic microorganisms (Eq. 1).

**Fig. 6.**

*4.2. Effect of substrate loads on microbial community profile in the anoxic BTF performance*

Changes in microbial community profile were observed every time operational conditions were changed. Increase of both $H_2S$ and $NO_3^-$ ILs in phase P3 led to the appearance of new DGGE bands from day 84 onwards (Fig. 5) representing *Brevundimonas* sp., *Rhodocyclales* bacterium and *Bacteroidetes* bacterium which are known heterotrophic denitrifiers [32]. These microorganisms could compete for $NO_3^-$ as electron acceptor with autotrophic denitrifiers in the anoxic BTF resulting in the decrease of $H_2S$ RE in the end of phase P3 (Fig. 2d). Huang et al. who studied the microbial community structure in five continuous stirred tank reactors [33] and three anaerobic sludge blanket reactors [34] for mixotrophic denitrifying sulfide removal also observed that microbial community was different at different $NO_3^-$ and acetate ILs applied. Huang et al. [33,34] reported that the optimized N/S molar ratio of 1.2 provided $S^0$ production of 75%, while the $SO_4^{2-}$ was the main product of sulfide oxidation when the reactors were fed with higher or lower inlet $NO_3^-$ and acetate loads (N/S ratio 0.4 and 1.8). Those studies [33,34] confirm our results: (i) the evolution of microbial community was due to the increase of $H_2S$ and $NO_3^-$ ILs from phase P2 to P3 (Table 2) and (ii) $H_2S$ oxidation to $S^0$ or $SO_4^{2-}$ was independent from N/S ratios, but related on $NO_3^-$ and $H_2S$ ILs, resulting in decreasing in $\%S^0$ production at the end of phase 3 which was likely caused by the insufficient $NO_3^-$ IL (Fig. 3).

*Thiobacillus* sp. was the only SO-NR bacterium observed in the BTF and therefore likely responsible for the simultaneous removal of $H_2S$ and $NO_3^-$ as described by Eq. (1) and (2).

Based on those equations, *Thiobacillus* sp. also produced biomass by using bicarbonate as carbon source under autotrophic denitrification as evidenced by lower carbon in the effluents than in the influents during phases P2-P4 (Fig. 3). *Stenotrophomonas* sp., a heterotrophic denitrifier detected since the first day of BTF operation, can survive by utilizing organic compounds excreted by autotrophs and microbial biomass ($C_5H_7O_2N$) produced during $H_2S$ oxidation via autotrophic denitrification (Eq. 1) [35]. Heterotrophic denitrifiers have also been detected from autotrophic systems, further verifying that their activity can be sustained by the organic material excreted by *Thiobacillus* sp. [36–38]. Fig. 3 shows that carbon was bound to the biomass during the BTF operation under autotrophic conditions, and carbon was released during period P5, when acetate was added to the feed, indicating degradation of the previously formed biomass.

*4.3. Effect of gas and liquid retention times on the BTF performance*

During BTF operation, a trickling liquid velocity (TLV) of 0.22 m $h^{-1}$ (flow rate of 2.5 L $h^{-1}$), $H_2S$ RE >95% was observed without any operational problems such as clogging and bed drying. The TLV applied to the BTF in this study was much lower than those used in several previous studies, while gas flow rates were similar (Table 1). TLV typically has a low impact on the $H_2S$ RE of anoxic BTFs as the electron acceptor ($NO_3^-$) is dissolved into the liquid phase [11,39], although high TLVs (>18.9 m $h^{-1}$) could severely impact the BTF performance by generating high pressure drops [27] as well as biomass detachment [40]. Biomass growth had a strong impact on the HRT of the BTF during the study. Based on the results of RTD tests, the HRT at the end of the study (day 139) was six times shorter than the initial HRT (day -16) (Fig. S2), while the gas retention time was less affected (Fig. S1). This suggests that the retention time of the liquid (synthetic nitrified wastewater) should be increased and optimized during BTF operation to maintain an optimal contact time between $NO_3^-$ in the liquid phase and $H_2S$ in the gas phase. The large decrease in the HRT during the study might

explain the $H_2S$ breakthrough observed at the end of phase P3 that required additional $NO_3^-$ to maintain high desulfurization efficiency (Fig. 2c and e). Conversely, the decrease of the EBRT from 3.5 to 2.9 min had less effect on the $H_2S$ RE compared to that of the HRT reduction. The EBRTs tested in this study were in the range of commonly reported values for BTF operation under both anoxic (Table 1) and aerobic [41,42] conditions. In a previous study involving mixtures of pollutants, Montebello et al. [30] reported that a decrease of the EBRT in an anoxic BTF had much less effect on the $H_2E$ RE than to the methylmercaptan ($CH_3SH$) RE due to the higher solubility of $H_2S$ compared to that of $CH_3SH$.

*4.4. Practical implications*

The results from this study showed that $H_2S$ removal could be achieved in an anoxic BTF using nitrified/$NO_3^-$-contaminated wastewater as an electron acceptor. The anoxic BTF can be applied for biogas cleaning prior to $CO_2$ removal step or used in combined heat and power (CHP) unit without $CH_4$ dilution as $N_2$ and $CO_2$ production was not significant in the system. This study suggested that the BTF can be operated with wastewater containing organic carbon (C/N molar ratio of 0.2) as it is beneficial to increase the $NO_3^-$ RE via mixotrophic denitrification and provides $CO_2$ as the endogenous carbon source instead of adding an external bicarbonate buffer [31]. However, the $NO_3^-$ IL should be optimized to serve sufficiently for both autotrophic and heterotrophic denitrifiers.

Acetate is a readily biodegradable organic carbon source that was chosen as a model organic compound in this study because it is easily available and measured. However, much more recalcitrant and slowly biodegradable organic matter would likely be available in the nitrified wastewater after aerobic oxidation. The presence of poorly soluble organic matter in the BTF may hamper gas/liquid mass transfer and the SO-NR activity, resulting in low $H_2S$ and $NO_3^-$ removal. Therefore, additional research on the effects of slowly biodegradable organic matter on BTF operation is therefore required.

## 5. Conclusions

Anoxic BTF operation under completely autotrophic conditions resulted in a maximum $H_2S$ EC of 19.2 g S $m^{-3}$ $h^{-1}$ (>99% RE), at inlet $NO_3^-$ loading rates ranging from 2.9 to12.9 $NO_3^-$-N $m^{-3}$ $h^{-1}$ (N/S ratios = 1.2-1.7 mol $mol^{-1}$). Mixotrophic operation (C/N ratio=0.2) stimulated the growth and activity of heterotrophic denitrifiers in the BTF. Biomass accumulation in the filter bed caused a reduction of the HRT, leading to insufficient $NO_3^-$ supply for oxidizing $H_2S$. From a practical viewpoint, the anoxic BTF should be operated at TLVs > 0.22 m $h^{-1}$ during long-term operation to enhance $NO_3^-$ distribution in the filter bed.

## 6. Acknowledgement

This research was supported by the Marie Skłodowska-Curie European Joint Doctorate (EJD) *Advanced Biological Waste-To-Energy Technologies* (ABWET) funded by the European Union's Horizon 2020 research and innovation programme [grant number 643071].

## 7. References

[1] D. Pokorna, J. Zabranska, Sulfur-oxidizing bacteria in environmental technology, Biotechnol. Adv. 33 (2015) 1246–1259. doi:10.1016/j.biotechadv.2015.02.007.

[2] J. Kanjanarong, B.S. Giri, D.P. Jaisi, F.R. Oliveira, P. Boonsawang, S. Chaiprapat, R.S. Singh, A. Balakrishna, S.K. Khanal, Removal of hydrogen sulfide generated during anaerobic treatment of sulfate-laden wastewater using biochar: Evaluation of efficiency and mechanisms, Bioresour. Technol. 234 (2017) 115–121. doi:10.1016/j.biortech.2017.03.009.

[3] US Occupational Safety and Health Administration (OSHA), Fact sheet: Hydrogen sulfide. https://www.osha.gov/OshDoc/data_Hurricane_Facts/hydrogen_sulfide_fact.html, 2005. (accessed 21 September 2017).

[4] G. Soreanu, M. Béland, P. Falletta, K. Edmonson, P. Seto, Laboratory pilot scale study for $H_2S$ removal from biogas in an anoxic biotrickling filter, Water Sci. Technol. 57 (2008) 201–207. doi:10.2166/wst.2008.023.

[5] S.K. Khanal, Y. Li, Biogas Production and Applications, in: Y. Li, S.K. Khanal (Eds.), Bioenergy: Principle and Application, John Wiley & Sons, Inc., 2017: pp. 338–360.

[6] G. Soreanu, M. Béland, P. Falletta, B. Ventresca, P. Seto, Evaluation of different packing media for anoxic $H_2S$ control in biogas, Environ. Technol. 30 (2009) 1249–1259. doi:10.1080/09593330902998314.

[7] M. Fernández, M. Ramírez, J.M. Gómez, D. Cantero, Biogas biodesulfurization in an anoxic biotrickling filter packed with open-pore polyurethane foam, J. Hazard. Mater. 264 (2014) 529–535. doi:10.1016/j.jhazmat.2013.10.046.

[8] F. Almenglo, M. Ramírez, J.M. Gómez, D. Cantero, Operational conditions for start-up and nitrate-feeding in an anoxic biotrickling filtration process at pilot scale, Chem. Eng. J. 285 (2016) 83–91. doi:10.1016/j.cej.2015.09.094.

[9] M. Mora, M. Fernández, J.M. Gómez, D. Cantero, J. Lafuente, X. Gamisans, D. Gabriel, Kinetic and stoichiometric characterization of anoxic sulfide oxidation by SO-NR mixed cultures from anoxic biotrickling filters, Appl. Microbiol. Biotechnol. 99 (2014) 77–87. doi:10.1007/s00253-014-5688-5.

[10] F. Almenglo, M. Ramírez, J.M. Gómez, D. Cantero, X. Gamisans, A.D. Dorado, Modeling and control strategies for anoxic biotrickling filtration in biogas purification, J. Chem. Technol. Biotechnol. 91 (2016) 1782–1793. doi:10.1002/jctb.4769.

[11] L.R. López, J. Brito, M. Mora, Fernando Almenglo, J.A. Baeza, M. Ramírez, J. Lafuente, D. Cantero, D. Gabriel, Feedforward control application in aerobic and anoxic biotrickling filters for $H_2S$ removalfrom biogas, J. Chem. Technol. Biotechnol. 93 (2018) 2307–2315. doi:DOI 10.1002/jctb.5575.

[12] X. Li, X. Jiang, Q. Zhou, W. Jiang, Effect of S/N ratio on the removal of hydrogen sulfide from biogas in anoxic bioreactors, Appl. Biochem. Biotechnol. 180 (2016) 930–944. doi:10.1007/s12010-016-2143-3.

[13] P.I. Cano, J. Colón, M. Ramírez, J. Lafuente, D. Gabriel, D. Cantero, Life cycle assessment of different physical-chemical and biological technologies for biogas desulfurization in sewage treatment plants, J. Clean. Prod. 181 (2018) 663–674. doi:10.1016/j.jclepro.2018.02.018.

[14] A.A. Forbis-Stokes, L. Rocha-Melogno, M.A. Deshusses, Nitrifying trickling filters and denitrifying bioreactors for nitrogen management of high-strength anaerobic digestion effluent, Chemosphere. 204 (2018) 119–129. doi:10.1016/j.chemosphere.2018.03.137.

[15] P.G. Hunt, K.C. Stone, T.A. Matheny, M.E. Poach, M.B. Vanotti, T.F. Ducey, Denitrification of nitrified and non-nitrified swine lagoon wastewater in the suspended sludge layer of treatment wetlands, Ecol. Eng. 35 (2009) 1514–1522. doi:10.1016/j.ecoleng.2009.07.001.

[16] J. Qian, H. Lu, F. Jiang, G.A. Ekama, G.H. Chen, Beneficial co-treatment of simple wet flue gas desulphurization wastes with freshwater sewage through development of mixed denitrification-SANI process, Chem. Eng. J. 262 (2015) 109–118. doi:10.1016/j.cej.2014.09.066.

[17] F. Jiang, L. Zhang, G.L. Peng, S.Y. Liang, J. Qian, L. Wei, G.H. Chen, A novel approach to realize SANI process in freshwater sewage treatment - Use of wet flue gas desulfurization waste streams as sulfur source, Water Res. 47 (2013) 5773–5782. doi:10.1016/j.watres.2013.06.051.

[18] G. Zou, S. Papirio, A.-M. Lakaniemi, S.H. Ahoranta, J.A. Puhakka, High rate autotrophic denitrification in fluidized-bed biofilm reactors, Chem. Eng. J. 284 (2016)

1287–1294. doi:10.1016/j.cej.2015.09.074.

[19] R. Khanongnuch, F. Di Capua, A.-M. Lakaniemi, E.R. Rene, P.N.L. Lens, Experimental and artificial neural network (ANN) analysis of an anoxic sulfur oxidizing moving bed biofilm reactor (MBBR) under nitrate limiting conditions, Unpublished results (2018).

[20] H.S. Fogler, Elements of chemical reaction engineering, 5th ed., Prentice Hall, Indiana, 2016.

[21] R. Khanongnuch, F. Di Capua, A.-M. Lakaniemi, E.R. Rene, P.N.L. Lens, Effect of N/S ratio on anoxic thiosulfate oxidation in a fluidized bed reactor: experimental and artificial neural network model analysis, Process Biochem. 68 (2018) 171–181. doi:https://doi.org/10.1016/j.procbio.2018.02.018.

[22] D. Villa-Gomez, H. Ababneh, S. Papirio, D.P.L. Rousseau, P.N.L. Lens, Effect of sulfide concentration on the location of the metal precipitates in inversed fluidized bed reactors, J. Hazard. Mater. 192 (2011) 200–207. doi:10.1016/j.jhazmat.2011.05.002.

[23] APHA/AWWA/WEF, Standard methods for the examination of water and wastewater, 20th ed., American Public Health Association/American Water Works Association/Water Environment Federation, Washington D.C., 1999.

[24] T. Eregowda, L. Matanhike, E.R. Rene, P.N.L. Lens, Performance of a biotrickling filter for anaerobic utilization of gas-phase methanol coupled to thiosulphate reduction and resource recovery through volatile fatty acids production, Bioresour. Technol. 263 (2018) 591–600. doi:10.1016/j.biortech.2018.04.095.

[25] S. Kim, M.A. Deshusses, Development and experimental validation of a conceptual model for biotrickling filtration of $H_2S$, Environ. Prog. 22 (2003) 119–128. doi:10.1002/ep.670220214.

[26] F. Almenglo, T. Bezerra, J. Lafuente, D. Gabriel, M. Ramírez, D. Cantero, Effect of

gas-liquid flow pattern and microbial diversity analysis of a pilot-scale biotrickling filter for anoxic biogas desulfurization, Chemosphere. 157 (2016) 215–223. doi:10.1016/j.chemosphere.2016.05.016.

[27] M. Fernández, M. Ramírez, R.M. Pérez, J.M. Gómez, D. Cantero, Hydrogen sulphide removal from biogas by an anoxic biotrickling filter packed with Pall rings, Chem. Eng. J. 225 (2013) 456–463. doi:10.1016/j.cej.2013.04.020.

[28] M. Ben Jaber, A. Couvert, A. Amrane, P. Le Cloirec, E. Dumont, Hydrogen sulfide removal from a biogas mimic by biofiltration under anoxic conditions, J. Environ. Chem. Eng. 5 (2017) 5617–5623. doi:10.1016/j.jece.2017.10.029.

[29] F. Di Capua, S.H. Ahoranta, S. Papirio, P.N.L. Lens, G. Esposito, Impacts of sulfur source and temperature on sulfur-driven denitrification by pure and mixed cultures of *Thiobacillus*, Process Biochem. 51 (2016) 1576–1584. doi:10.1016/j.procbio.2016.06.010.

[30] A.M. Montebello, M. Fernández, F. Almenglo, M. Ramírez, D. Cantero, M. Baeza, D. Gabriel, Simultaneous methylmercaptan and hydrogen sulfide removal in the desulfurization of biogas in aerobic and anoxic biotrickling filters, Chem. Eng. J. 200–202 (2012) 237–246. doi:10.1016/j.cej.2012.06.043.

[31] A. Bayrakdar, E. Tilahun, B. Calli, Biogas desulfurization using autotrophic denitrification process, Appl. Microbiol. Biotechnol. 100 (2016) 939–948. doi:10.1007/s00253-015-7017-z.

[32] T. Tsubouchi, S. Koyama, K. Mori, Y. Shimane, K. Usui, M. Tokuda, A. Tame, K. Uematsu, T. Maruyama, Y. Hatada, *Brevundimonas denitrificans* sp. nov., a denitrifying bacterium isolated from deep subseafloor sediment, Int. J. Syst. Evol. Microbiol. 64 (2014) 3709–3716. doi:10.1099/ijs.0.067199-0.

[33] C. Huang, Z.-L. Li, F. Chen, Q. Liu, Y.-K. Zhao, J.-Z. Zhou, A.-J. Wang, Microbial

community structure and function in response to the shift of sulfide/nitrate loading ratio during the denitrifying sulfide removal process, Bioresour. Technol. 197 (2015) 227–234. doi:10.1016/j.biortech.2015.08.019.

[34] C. Huang, Q. Liu, C. Chen, F. Chen, Y.-K. Zhao, L.-F. Gao, W.-Z. Liu, J.-Z. Zhou, Z.-L. Li, A.-J. Wang, Elemental sulfur recovery and spatial distribution of functional bacteria and expressed genes under different carbon/nitrate/sulfide loadings in up-flow anaerobic sludge blanket reactors, J. Hazard. Mater. 324 (2017) 48–53. doi:10.1016/j.jhazmat.2016.03.024.

[35] B. Huber, B. Herzog, J.E. Drewes, K. Koch, E. Müller, Characterization of sulfur oxidizing bacteria related to biogenic sulfuric acid corrosion in sludge digesters, BMC Microbiol. 16 (2016) 1–11. doi:10.1186/s12866-016-0767-7.

[36] F. Di Capua, A.-M. Lakaniemi, J.A. Puhakka, P.N.L. Lens, G. Esposito, High-rate thiosulfate-driven denitrification at pH lower than 5 in fluidized-bed reactor, Chem. Eng. J. 310 (2017) 282–291. doi:10.1016/j.cej.2016.10.117.

[37] F. Di Capua, I. Milone, A.-M. Lakaniemi, E.D. van Hullebusch, P.N.L. Lens, G. Esposito, Effects of different nickel species on autotrophic denitrification driven by thiosulfate in batch tests and a fluidized-bed reactor, Bioresour. Technol. 238 (2017) 534–541. doi:10.1016/j.biortech.2017.04.082.

[38] F. Di Capua, I. Milone, A.-M. Lakaniemi, P.N.L. Lens, G. Esposito, High-rate autotrophic denitrification in a fluidized-bed reactor at psychrophilic temperatures, Chem. Eng. J. 313 (2017) 591–598. doi:10.1016/j.cej.2016.12.106.

[39] J. Brito, F. Almenglo, M. Ramírez, J.M. Gómez, D. Cantero, PID control system for biogas desulfurization under anoxic conditions, J. Chem. Technol. Biotechnol. (2017). doi:10.1002/jctb.5243.

[40] M. Fortuny, X. Gamisans, M.A. Deshusses, J. Lafuente, C. Casas, D. Gabriel,

Operational aspects of the desulfurization process of energy gases mimics in biotrickling filters, Water Res. 45 (2011) 5665–5674. doi:10.1016/j.watres.2011.08.029.

[41] B. Charnnok, T. Suksaroj, P. Boonswang, S. Chaiprapat, Oxidation of hydrogen sulfide in biogas using dissolved oxygen in the extreme acidic biofiltration operation, Bioresour. Technol. 131 (2013) 492–499. doi:10.1016/j.biortech.2012.12.114.

[42] M. Tomas, M. Fortuny, C. Lao, D. Gabriel, J. Lafuente, X. Gamisans, Technical and economical study of a full-scale biotrickling filter for $H_2S$ removal from biogas, Water Pract. Technol. 4 (2009). doi:10.2166/wpt.2009.026.

**List of figure captions**

**Fig. 1.** Schematic of the anoxic biotrickling filter for $H_2S$ removal. Dotted and continuous lines represent the gas and liquid flows, respectively.

**Fig. 2.** Time course profiles of influent and effluent pH, alkalinity, $H_2S$, $S^{2-}$, $SO_4^{2-}$, $S_2O_3^{2-}$, $NO_3^-$, $NO_2^-$ and acetate concentrations and removal efficiency (RE) of $H_2S$ and $NO_3^-$ in the anoxic biotrickling filter.

**Fig. 3.** N/S ratios and the mass balances of sulfur, nitrogen and carbon during BTF operation. % $S^0$ production and % carbon consumed in the BTF was based on the influent and effluent concentrations of sulfur or carbon, while % $N_2$ production was estimated from $NO_3^-$ and $NO_2^-$ in the liquid phase.

**Fig. 4.** Elimination capacities (EC) of $H_2S$ and $NO_3^-$ during different experimental phases (P1-P5) of anoxic biotrickling filter operation.

**Fig. 5.** Denaturing gradient gel electrophoresis (DGGE) profiles (left) and identification of the sequenced DGGE bands (right) of the biomass samples collected during the BTF operation.

**Fig. 6.** Profiles of sulfide ($S^{2-}$), nitrate ($NO_3^-$), nitrite ($NO_2^-$) and sulfate ($SO_4^{2-}$) concentrations in the batch activity tests with biofilm-attached PUF cubes collected from the BTF on days 83 (a), 108 (b) and 137 (c and d; with and without acetate addition, respectively).

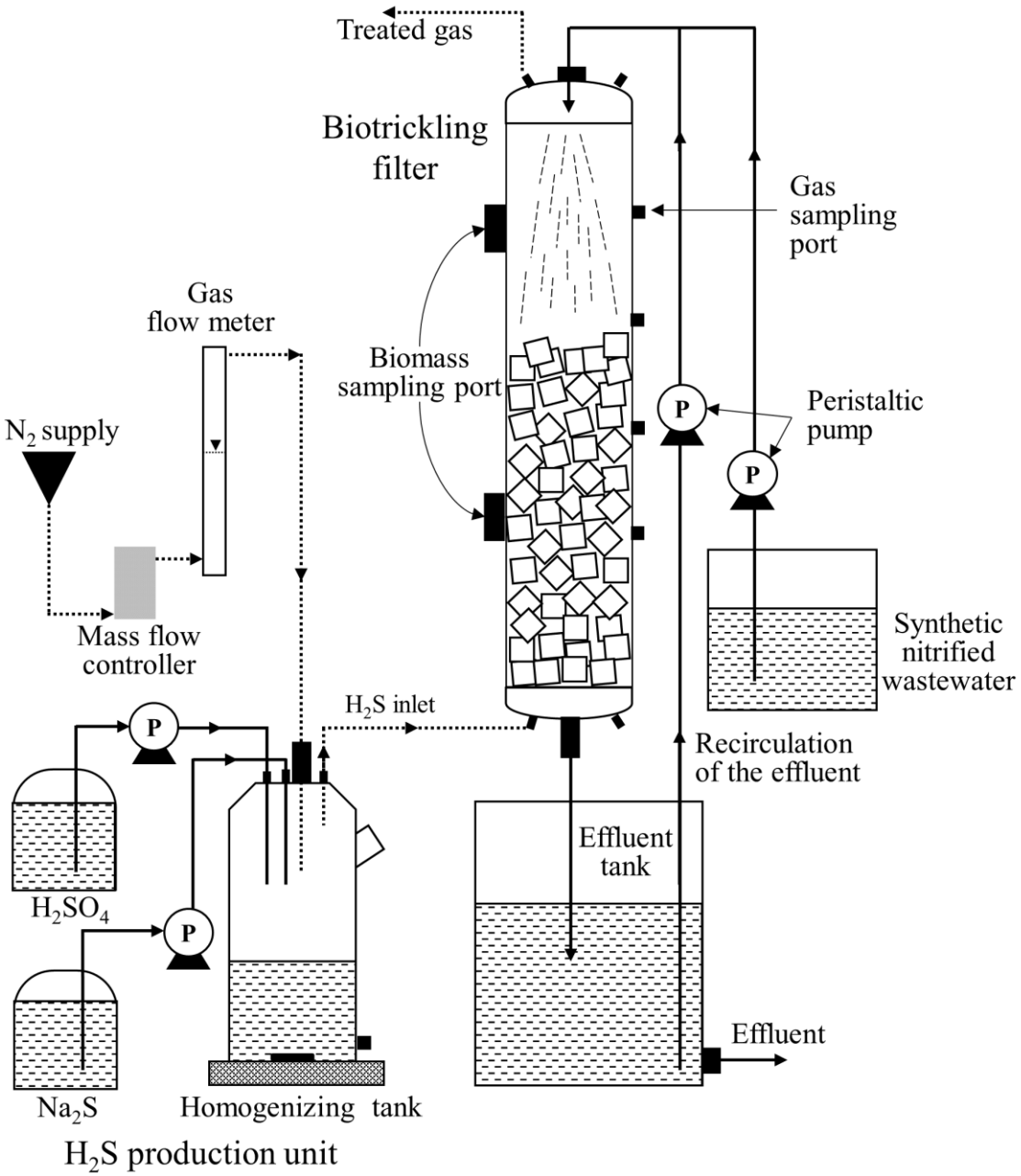
Treated gas
Biotrickling filter
Gas sampling port
Gas flow meter
Biomass sampling port
Peristaltic pump
$N_2$ supply
Mass flow controller
Synthetic nitrified wastewater
$H_2S$ inlet
Recirculation of the effluent
Effluent tank
$H_2SO_4$
Effluent
$Na_2S$
Homogenizing tank
$H_2S$ production unit

**Fig. 1.**

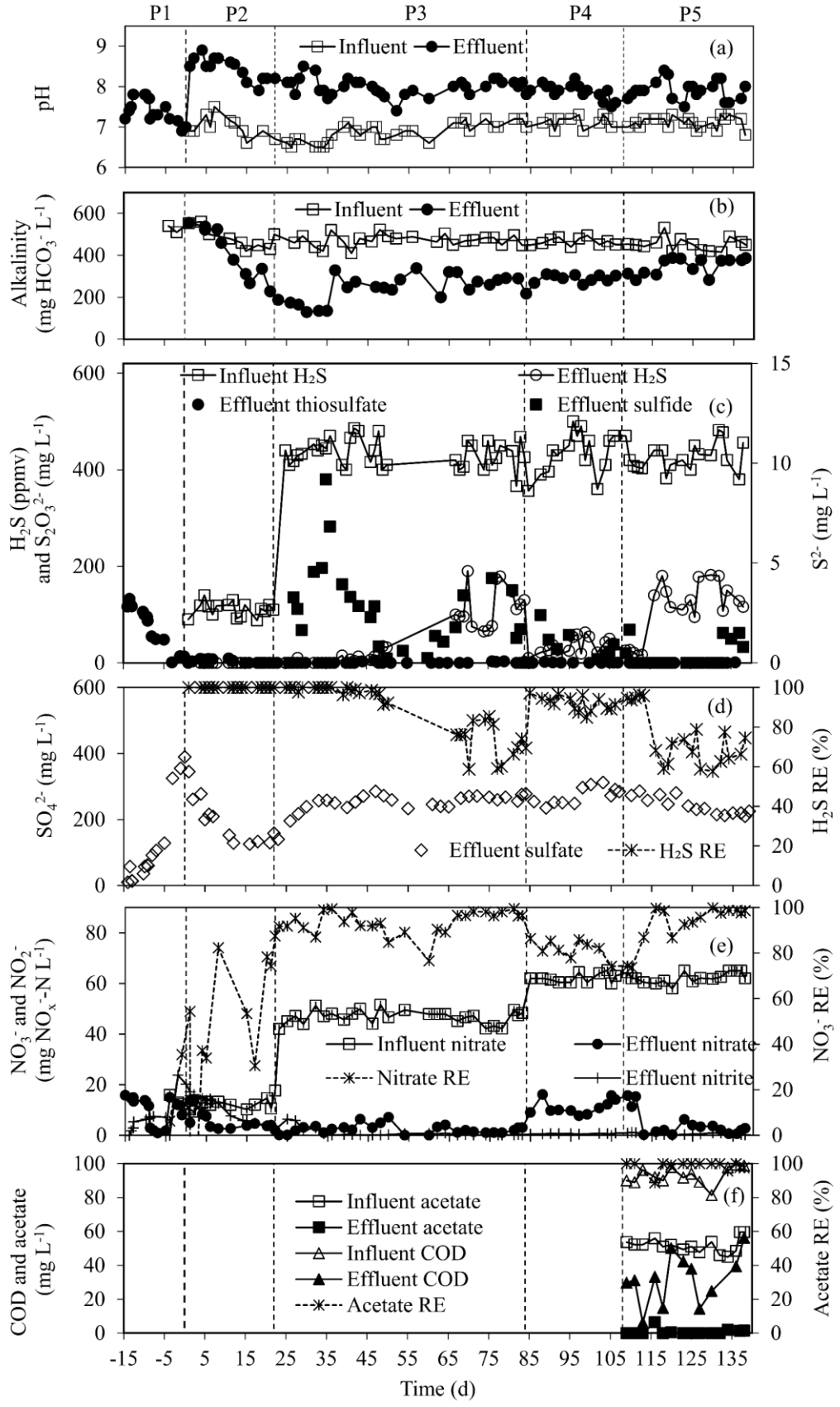
P1
P2
P3
P4
P5
pH
Influent
Effluent
(a)
Alkalinity (mg HCO3- L-1)
(b)
H2S (ppmv) and S2O32- (mg L-1)
Influent H2S
Effluent H2S
Effluent thiosulfate
Effluent sulfide
(c)
S2- (mg L-1)
SO42- (mg L-1)
(d)
Effluent sulfate
H2S RE
H2S RE (%)
NO3- and NO2- (mg NOx-N L-1)
(e)
Influent nitrate
Effluent nitrate
Nitrate RE
Effluent nitrite
NO3- RE (%)
COD and acetate (mg L-1)
(f)
Influent acetate
Effluent acetate
Influent COD
Effluent COD
Acetate RE
Acetate RE (%)
Time (d)

**Fig. 2.**

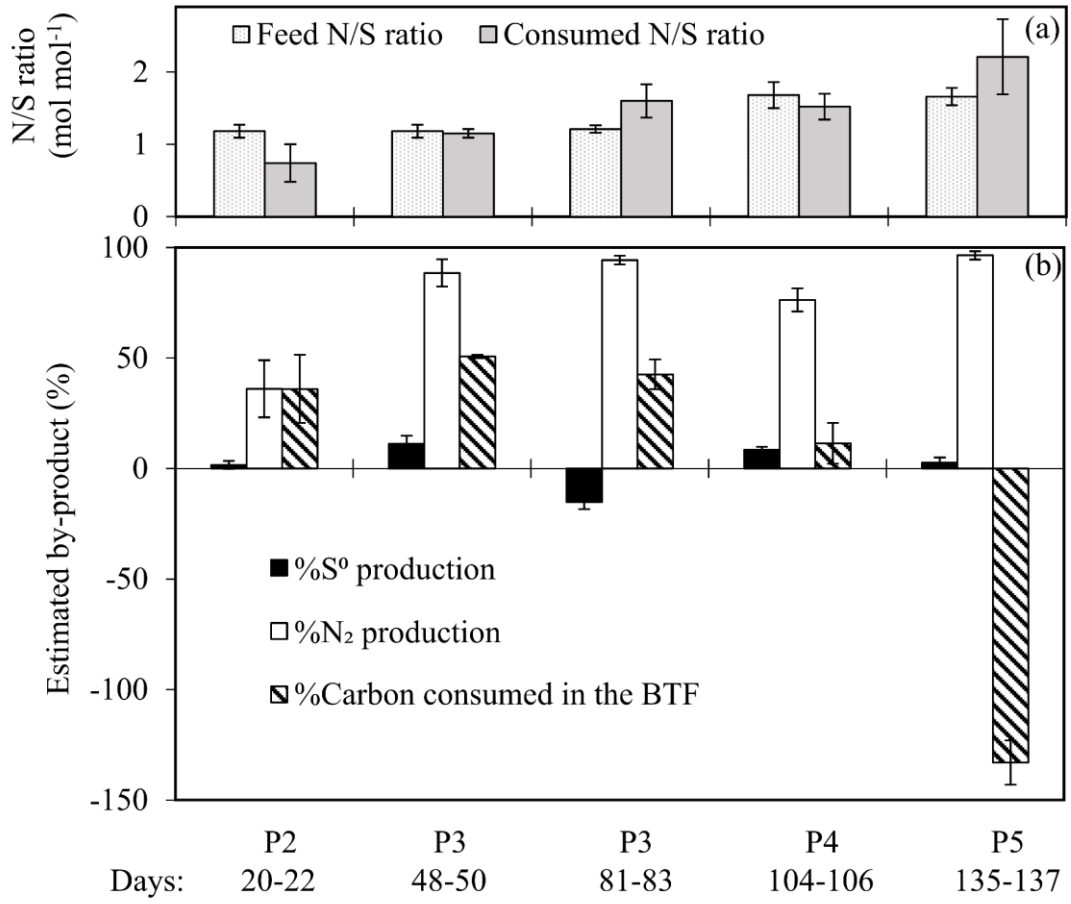
N/S ratio (mol mol-1)
Feed N/S ratio
Consumed N/S ratio
(a)
2
1
0
100
50
0
-50
-100
-150
(b)
Estimated by-product (%)
%S⁰ production
%N₂ production
%Carbon consumed in the BTF
P2
P3
P3
P4
P5
Days:
20-22
48-50
81-83
104-106
135-137

**Fig. 3.**

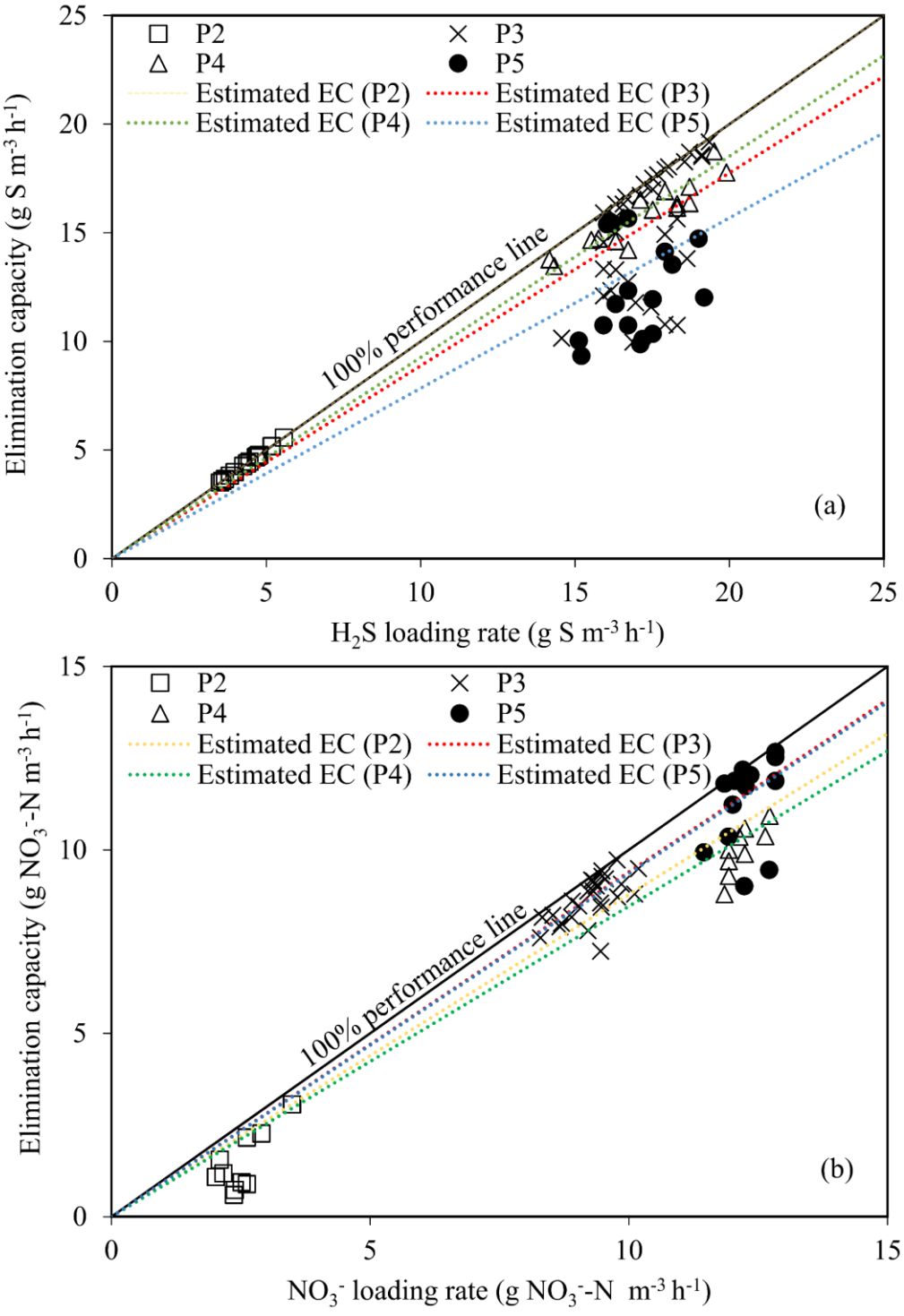
P2
P3
P4
P5
Estimated EC (P2)
Estimated EC (P3)
Estimated EC (P4)
Estimated EC (P5)
100% performance line
Elimination capacity (g S m-3 h-1)
H2S loading rate (g S m-3 h-1)
(a)
Elimination capacity (g NO3--N m-3 h-1)
NO3- loading rate (g NO3--N m-3 h-1)
(b)

**Fig. 4.**

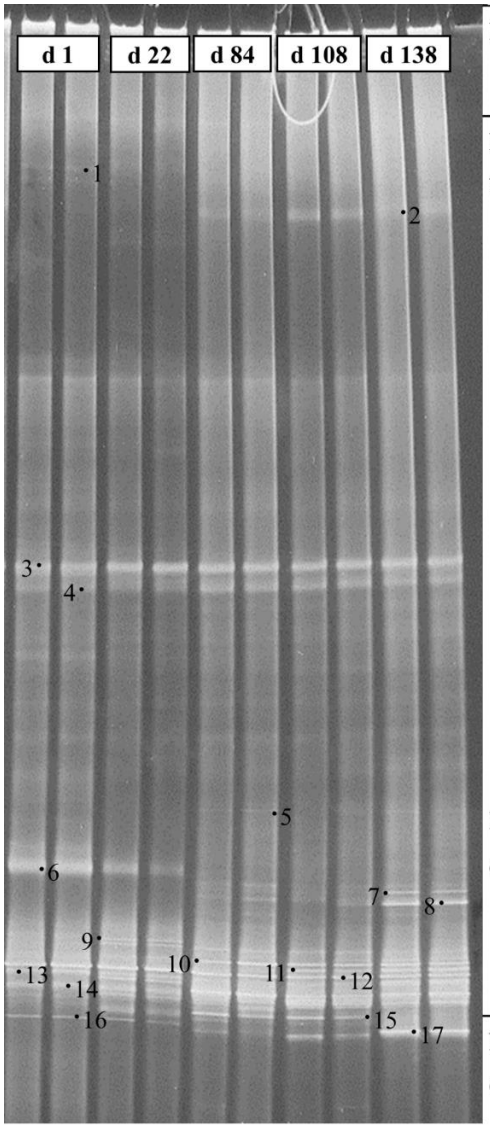


| Phylum | Class/order/family | Affiliation[b] | Band(s)[a] | Accession number | Similarity (%) | Sequence length |
|---|---|---|---|---|---|---|
| Proteo-bacteria | *β*/Nitrosomonadales/ Thiobacillaceae | *Thiobacillus* sp. | 1, 9, 10, 12, 13, 16 | KM200026.1, JX530173.1, KM200014.1 | 98.0-100 | 433-508 |
| | *β*/Rhodocyclales | *Rhodocyclales* bacterium | 11 | JQ723653.1 | 98.7 | 448 |
| | *β* | Uncultured *β* proteobacterium | 5 | AY133108.1 | 92.6 | 448 |
| | *α*/Caulobacterales/ Caulobacteraceae | *Brevundimonas* sp. | 2 | EF590244.1 | 100 | 425 |
| | *α*/Rhodobacterales/ Rhodobacteraceae | *Rhodobacter* sp. | 4, 15, 17 | LN879886.1, JN648234.1 | 92.6-99.1 | 415-429 |
| | *γ*/Xanthomonadales/ Xanthomonadaceae | *Stenotrophomonas* sp. | 3, 14 | KY490132.1, KM021209.1 | 91.8-94.5 | 456-510 |
| Bacteroi detes | Flavobacteriia/Flavobacteriales/ Flavobacteriaceae | *Chryseobacterium* sp. | 6 | JQ724341.1 | 99.8 | 485 |
| | - | *Bacteroidetes*/*Chlorobi* group bacterium | 7, 8 | KU685184.1, LN998004.1 | 96.2-96.3 | 416-418 |

Note: d= day, [a] Band label of DGGE-separated DNA fragments, and [b] Closet relative DGGE-separated DNA fragment in Genbank

**Fig. 5.**

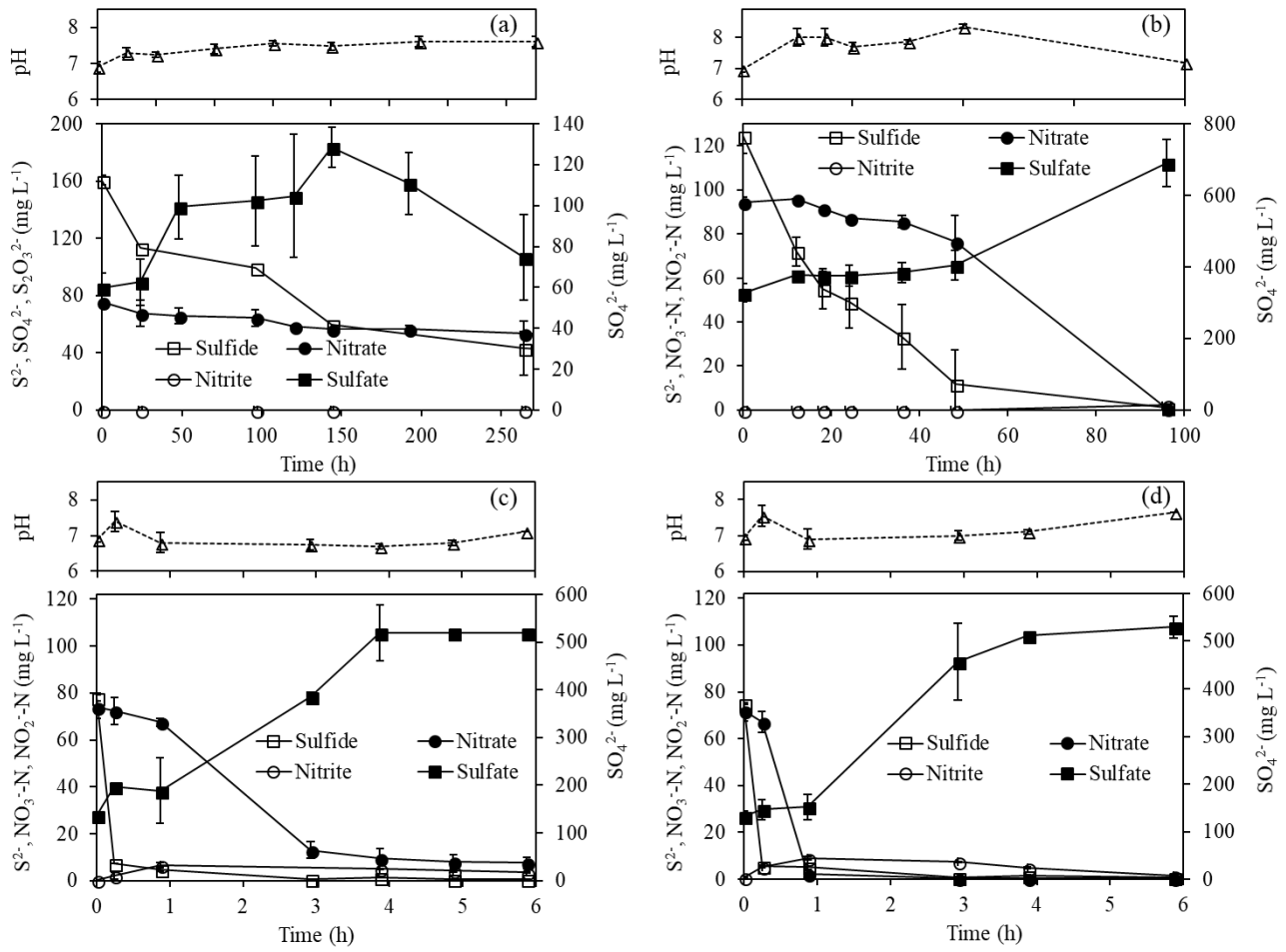
(a)
(b)
(c)
(d)
pH
Time (h)
Sulfide
Nitrate
Nitrite
Sulfate
$S^{2-}$, $SO_4^{2-}$, $S_2O_3^{2-}$ (mg $L^{-1}$)
$S^{2-}$, $NO_3^-$-N, $NO_2^-$-N (mg $L^{-1}$)
$SO_4^{2-}$ (mg $L^{-1}$)

**Fig. 6.**

**Table 1.** $H_2S$ removal selected anoxic biofilter/biotrickling filter studies conducted at different operational parameters.

| Packing materials | Bed volume (L) | EBRT (min) | $H_2S$ ($ppm_v$) | $H_2S$ IL[b] (g S $m^{-3}$ $h^{-1}$) | The maximum EC[b] (g S $m^{-3}$ $h^{-1}$) | Gas flow rate (L $h^{-1}$) | $NO_3^-$ (mg $L^{-1}$) | Trickling velocity (m $h^{-1}$) | N/S ratio | pH of Liquid medium | Temperature (°C) | References |
|---|---|---|---|---|---|---|---|---|---|---|---|---|
| Plastic fiber | 12.0 | 5-16 | 1000-4000 | 1-31 | 11.7 | 25-75 | 300-1800[c] | 1.7 | N.D.[d] | 6.5 | 23±2 | [4] |
| Pall rings | 2.40 | 2-17 | 1400-14600 | 9-201 | 170 | 8.4-60 | 50-600[c] | 2.3-20.6 | 0.7-1.5 | 7.0 | 29 ±1 | [27] |
| OPUF[a] | 2.40 | 2-6 | 850-8500 | 6-201 | 170 | 60 | 500-2400[c] | 2.3-20.6 | 0.4-1.6 | 7.3-7.5 | 15-36 | [7] |
| Concrete waste | 7.85 | 1-5 | 25-1100 | 2-38 | 30.3 | 94-470 | N.D.[d] | 0.01[e] | 0.4-1.6 | 7.0-9.0 | N.D.[d] | [28] |
| PUF[a] | 2.11 | 3.5 | 100-500 | 3-20 | 19.2 | 60 | 12-64 | 0.22 | 1.2-1.7 | 7.0±2.0 | 24±2 | This study |

Note: [a] OPUF and PUF = open-polyurethane foam and polyurethane foam, respectively

[b] IL and EC = inlet loading rate and elimination capacity, respectively

[c] Fresh $NO_3^-$ was supplied once after $NO_3^-$ in liquid medium was completely consumed

[d] N.D. = no data available

[e] the liquid was trickled for 5 min each hour

**Table 2.** Operational and influent characteristics during different phases of the biotrickling filter operation.

| Phase | P1 | P2 | P3 | P4 | P5 |
|---|---|---|---|---|---|
| Time (days) | -15-0 | 1-22 | 23-84 | 85-108 | 109-138 |
| Feeding mode | Batch | Continuous | Continuous | Continuous | Continuous |
| $H_2S$ ($ppm_v$) | - | 111 (±15) | 434 (±28) | 433 (±44) | 428 (±30) |
| IL[a] ($g\ S\ m^{-3}\ h^{-1}$) | - | 3.5-5.6 | 14.6-19.3 | 14.2-20.0 | 15.1-19.2 |
| $S_2O_3^{2-}$-S ($mg\ S\ L^{-1}$) | 67.4 (±8.4) | - | - | - | - |
| $NO_3^-$-N ($mg\ N\ L^{-1}$) | 15.5 (±1.0) | 12.2 (±2.1) | 46.9 (±2.6) | 62.2 (±1.8) | 62.1 (±2.0) |
| IL[a] ($g\ N\ m^{-3}\ h^{-1}$) | - | 1.8-2.9 | 8.3-10.2 | 11.8-12.9 | 11.4-15.0 |
| $CH_3COO^-$ ($mg\ L^{-1}$) | - | - | - | - | 51.4 (±2.8) |
| Feed N/S ratio ($mol\ mol^{-1}$) | 0.53 (±0.01) | 1.18 (±0.09) | 1.21 (±0.05) | 1.68 (±0.18) | 1.66 (±0.12) |

Note: [a] IL inlet loading rate

**Table 3.** Specific sulfide and nitrate removal rate of biomass-attached polyurethane foam (PUF) cubes in the batch activity tests.

| Day[a] | No. | Initial concentrations | | | Specific removal rates | |
|---|---|---|---|---|---|---|
| | | $S^{2-}$ (mg S $L^{-1}$) | $NO_3^-$-N (mg N $L^{-1}$) | $CH_3COO^-$ (mg $L^{-1}$) | $S^{2-}$ (g S $m^{-3}_{PUF}$ $h^{-1}$) | $NO_3^-$ (g N $m^{-3}_{PUF}$ $h^{-1}$) |
| 83 | I | 161 (±16) | 75.5 (±1.1) | - | 9.6 (±1.2) | 1.8 (±0.4) |
| 108 | II | 124 (±8) | 94.5 (±2.1) | - | 25.9 (±4.0) | 23.1 (±3.2) |
| 137 | III | 78.2 (±1.7) | 74.1 (±5.0) | - | 1131 (±10) | 359 (±52) |
| 137 | IV | 75.0 (±0.2) | 72.1 (±4.4) | 52.5 (±3.5) | 1061 (±35) | 1400 (±57) |

Note: [a] day of biomass harvesting